Evoked and Intrinsic Asymmetries during Auditory Attention: Implications for the Contralateral and Neglect Models of Functioning

Terri M. Teshiba[1,2], Josef Ling[1], David A. Ruhl[1], Bronwyn S. Bedrick[1], Amanda Peña[1] and Andrew R. Mayer[1,3]

[1]The Mind Research Network and Lovelace Biomedical and Environmental Research Institute, Albuquerque, NM 87106, USA, [2]Center for Neurobehavioral Genetics, Semel Institute for Neuroscience and Human Behavior, University of California, Los Angeles, CA 90095, USA and [3]Neurology and Psychology Departments, University of New Mexico, Albuquerque, NM 87131, USA

Address correspondence to Andrew Mayer, PhD, The Mind Research Network, Pete & Nancy Domenici Hall, 1101 Yale Blvd. NE, Albuquerque, NM 87106, USA. Email: amayer@mrn.org.

Unlike the visual system, a direct mapping of extrapersonal space does not exist within human auditory cortex (AC). Thus, models (contralateral bias vs. neglect) of how auditory spatial attention is allocated remain debated, as does the role of hemispheric asymmetries. To further examine these questions, 27 participants completed an exogenous auditory orienting task while undergoing functional magnetic resonance imaging. Resting-state data were also collected to characterize intrinsic activity within the AC. Current results provide the first evidence of hemispheric specialization in the "where" (right secondary AC) auditory processing stream during both evoked (orienting task) and intrinsic (resting-state data) activity, suggesting that spontaneous and evoked activity may be synchronized by similar cortical hierarchies. Strong evidence for a contralateral bias model was observed during rapid deployment stages (facilitation) of auditory attention in bilateral AC. However, contralateral bias increased for left and decreased for right AC (neglect model) after longer stimulus onset asynchronies (inhibition of return), suggesting a role for higher-order cortical structures in modulating AC functioning. Prime candidates for attentional modulation include the frontoparietal network, which demonstrated right hemisphere lateralization across multiple attentional states.

Keywords: asymmetry, attention, auditory, connectivity, fMRI

Introduction

Identifying the spatial location of sudden acoustic stimuli is critical to everyday functioning. Auditory spatial localization involves a complex interplay between stimulus location (in right or left hemifield; i.e., lateralization) and differential involvement of left and right hemispheres (i.e., hemispheric asymmetries). A prominent theory suggests right temporoparietal areas set a global reference frame for auditory space, with more precise computation of spatial coordinates within different hemifields occurring in auditory cortex (AC) and subcortical structures (Spierer et al. 2009). Right temporoparietal dominance in auditory localization is generally supported by lesion (Tanaka et al. 1999; Bellmann et al. 2001) and some neuroimaging (Zatorre et al. 1999; Brunetti et al. 2008; Lewald et al. 2008) data. However, hemispheric asymmetries within AC during auditory spatial attention are more actively debated (Zatorre and Penhune 2001; Hine and Debener 2007; Gilmore et al. 2009), with 2 models principally supported.

The contralateral model (Fig. 1A) predicts that the AC in both hemispheres responds more strongly to contralateral relative to ipsilateral stimulation (Alho et al. 1999; Richter et al. 2009; Woods et al. 2009). Animal models suggest that contralateral bias may result from greater proportions of monaural and binaural neurons delivering excitatory input both directly from the cochlear nucleus and via brainstem nuclei to the contralateral AC and inhibitory input to the ipsilateral AC (Rouiller 1997; Woldorff et al. 1999). In contrast, an extension of the neglect model (Fig. 1B) predicts a strong contralateral bias in the left AC for right hemifield stimuli and more equal responses in the right AC to stimuli in both hemifields in the healthy brain (Mesulam 1999). The neglect model has received considerable support from both electrophysiological and hemodynamic imaging studies (Deouell et al. 1998; Kaiser et al. 2000; Krumbholz et al. 2007; Schonwiesner et al. 2007).

However, hemispheric asymmetries in AC may depend on different attentional states inherent in auditory spatial localization (e.g., facilitation at shorter stimulus onset asynchronies [SOA] vs. inhibition of attention to previously cued locations [inhibition of return, IOR] at longer SOA), task requirements (e.g., linguistic vs. nonlinguistic processing), stimulus presentation (e.g., monaural vs. binaural tones), or subregions within AC (primary vs. secondary AC). Moreover, there are several lines of research suggesting hemispheric differences in structural morphology. Specifically, both the acoustic radiation and the Heschl's gyrus (HG) are located more rostrally in the right compared with left hemisphere (Penhune et al. 1996; Rademacher et al. 2001), with a rostral and superior shift also present for the right superior temporal sulcus (Van Essen 2005). In contrast, greater volume for the left HG (Penhune et al. 1996) and planum temporale (PT) (Toga and Thompson 2003; Van Essen 2005) has been reported, although some of these differences may be partially attributable to differences in white matter volume or sulcal morphometry (Penhune et al. 1996; Westbury et al. 1999; Dorsaint-Pierre et al. 2006).

Not surprisingly, the few neuroimaging studies that have directly compared activity in homologous areas of both hemispheres provide inconsistent evidence of asymmetries within frontotemporoparietal attention areas and AC (Mayer et al. 2006; Petit et al. 2007; Krumbholz et al. 2009). Additionally, no studies have examined hemispheric asymmetries in functional connectivity magnetic resonance imaging (fcMRI) within AC during resting state (i.e., intrinsic neural activity). The resting brain is characterized by spontaneous neuronal fluctuations that synchronously occur over spatially distributed networks (Raichle and Mintun 2006), with these networks mirroring activity evoked across a variety of cognitive challenges (Smith et al. 2009). These resting-state fluctuations can be measured through low frequency changes in the blood oxygen level dependent response recorded while subjects rest passively in the scanner. A cross-hemisphere comparison of resting-state data would
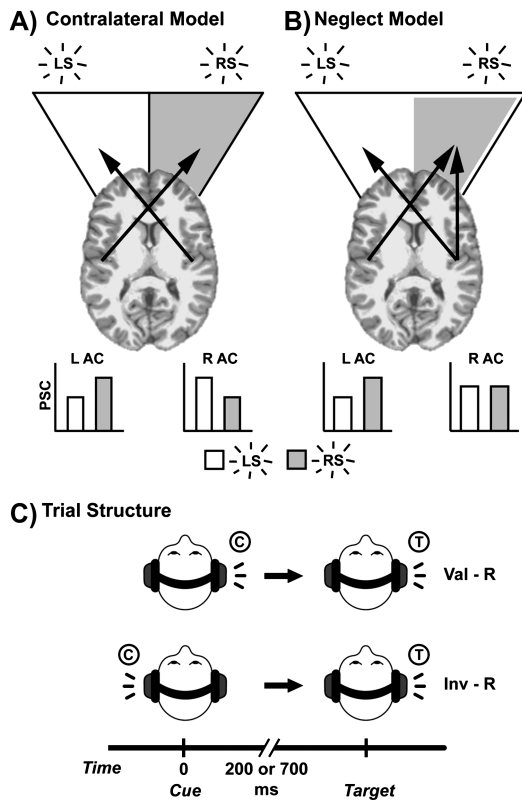
Figure 1. This figure presents predictions and cartoon illustrations of the contralateral (Panel A) and neglect (Panel B) models of response to lateralized auditory stimuli. In the contralateral model, both left and right hemispheres display a bias (arrows) toward stimuli in the contralateral hemifield. Bar graphs indicate hypothesized greater activation (PSC, percent signal change) to contralateral stimuli (LS, left stimulus; RS, right stimulus) within each AC (L AC, left auditory cortex; R AC, right auditory cortex). In the neglect model, the L AC shows a bias toward stimuli in the right hemifield (gray area), while the R AC responds more equally to stimuli in both hemifields (white area). Panel C presents the trial structure for sample valid (Val-R) and invalid right (Inv-R) trials. For valid trials, cue (C) and target (T) occur in same headphone/hemifield; for invalid trials, targets occur in opposite headphones/hemifields.

provide unique information regarding whether intrinsic activity in one hemisphere more strongly synchronizes activity in the other hemisphere independent of task-related demands.

The current study utilized functional magnetic resonance imaging (fMRI) to examine whether activation within primary (parcellated from high resolution T_1 images) and secondary AC was more consistent with the contralateral or neglect model during 2 separate attentional states (Mayer et al. 2007). Specifically, short cue–target intervals were chosen to evoke more rapid/adaptive attentional deployment (Dosenbach et al. 2007) within the AC, a state that is less likely to be influenced by higher order cortical networks. In addition, longer cue–target intervals result in IOR, representing a more controlled attentional state that is more likely regulated by higher order cortical sites. Separate analyses were also conducted to investigate effects of stimulus laterality (hemifield of presentation) versus hemispheric asymmetries (voxelwise comparisons) on evoked and intrinsic neural activity.

Experimental Procedures

Participants

Thirty-two right-handed adult volunteers (18 females, 26.5 ± 5.7 years old; 13.6 ± 2.5 years of education; mean Edinburgh Handedness Inventory = 95.4 ± 7.8, [Oldfield 1971]) participated in the current experiment. Subjects with a previous history of neurological disease, psychiatric disturbance, substance abuse, prescribed psychoactive medications, attention deficit hyperactivity disorder, or learning disorder were excluded from the study. All subjects had normal hearing according to self-report. One female subject was excluded from further analysis due to anomalies in data acquisition and another was excluded as an outlier based on excessive motion (greater than 3 standard deviations [SDs]). One other female and 2 male subjects were identified as poor performers on the auditory orienting task (less than 70% accuracy rate) and were also excluded from further analysis. This left a total of 27 subjects to be included in the final analyses for the current study. Written informed consent was obtained from all subjects according to institutional guidelines at the University of New Mexico.

Tasks

All participants completed an exogenous auditory orienting task and a resting-state scan while undergoing fMRI on a 3.0-T Siemens Trio scanner. During bottom-up or exogenous auditory orienting, cues predict target location at chance levels (50%), evoking automatic shifts of attention that are characterized by a biphasic response time (RT) pattern (Posner and Cohen 1984). At shorter SOA, RT is faster for validly compared with invalidly cued trials (i.e., facilitation), while at longer SOA, RT is faster for invalidly cued trials (i.e., IOR).

Participants rested supine in the scanner with their head secured by a forehead strap, with additional foam padding to limit head motion within the head coil. Presentation software (Neurobehavioral Systems) was used for stimulus presentation, synchronization of stimulus events with the MRI scanner, and recording of RT. Visual stimuli included a white fixation cross (visual angle = 1.02°) on a black background that was rear projected onto an opaque white Plexiglas projection screen using a Sharp XG-C50X LCD projector. Subjects were instructed to keep their eyes fixated on the cross throughout the task.

Auditory stimuli were presented via an Avotec Silent Scan 3100 Series system. A 100 ms monaural (right vs. left) tone pip (2000 Hz) served as a spatial cue that correctly (e.g., both cue and target occurred in right headphone) predicted the location of a second 100 ms monaural target tone pip (1000 Hz) on 50% of the experimental trials (i.e., on valid trials). Valid trials (Fig. 1C) involve the covert shifting of attentional resources following the cue and the detection of targets following a delay (both stimuli presented to a single hemifield). On the remainder of the trials (i.e., invalid trials), the cue incorrectly predicted target location. Therefore, whereas the cue and target occurred in the same hemifield for validly cued trials, both hemifields were stimulated during invalid trials (e.g., cue occurred in right headphone/hemifield followed by target in left headphone/hemifield). The laterality for the stimulus presentation in each trial was operationally defined based on the location of the target, consistent with conventions established in previous cueing studies (Mangun et al. 1994; Corbetta et al. 2000; Shulman et al. 2010). In addition to attentional shifting and target detection, invalid trials (Fig. 1C) also involve the reorienting of attentional resources following the appearance of a target in the uncued hemifield.

Participants were informed that the cues did not contain any useful information about the location of the target prior to the

start of the experiment. Both tones were sampled with a 10 ms linear onset–offset ramp to reduce the occurrence of clicks during auditory stimulus presentation. Measurement of decibel levels indicated no differences between the left and the right headphones for both the 1000 and 2000 Hz tones. Stimulus onset asynchrony between cue and target (200 or 700 ms), trial validity, and laterality (left or right target) were pseudorandomly varied throughout the experiment. The intertrial interval was jittered between 4, 6, or 8 s to both facilitate sampling of the hemodynamic response (Burock et al. 1998) and minimize the likelihood of nonlinear summing of hemodynamic responses (Glover 1999).

Participants were instructed to make a key press with their right index finger for targets appearing in the left headphone and right middle finger for targets appearing in the right headphone. A total of 21 trials for each of the 8 conditions (valid or invalid, 200 or 700 ms SOA, left or right target) were presented across 3 separate imaging runs. RT was measured from the onset of the target stimulus to the completion of a key-press response. Participants practiced the task and were required to demonstrate 100% proficiency in verbally identifying the cue compared with the target tone pips before entering the scanner environment.

Intrinsic fluctuations in neuronal activity (Fox et al. 2005) were measured during an extended resting-state task. Specifically, participants maintained visual fixation on a white cross centered on a black background (visual angle = $1.54°$) for approximately 5 min.

MR Imaging
High-resolution T_1-weighted anatomic images were acquired with a 5-echo multiecho magnetization prepared rapid gradient echo sequence (echo time [TE] = 1.64, 3.5, 5.36, 7.22, and 9.08 ms, repetition time [TR] = 2.53 s, inversion time = 1.2 s, 7° flip angle, number of excitations = 1, slice thickness = 1 mm, field of view (FOV) = 256 mm, resolution = 256 × 256]. For the 3 fMRI series and the functional connectivity data, echo-planar images were collected (162 for orienting task runs, 150 for resting-state run) using a single-shot gradient-echo echo-planar pulse sequence (TR = 2000 ms; TE = 29 ms; flip angle = 75°; FOV = 240 mm; matrix size = 64 × 64). The first image of each run was eliminated to account for T_1 equilibrium effects, leaving a total of 483 images for the final analyses of orienting tasks and 149 for the resting state run.

Auditory Orienting Task: Image Processing and Statistical Analyses
Functional images were generated using Analysis of Functional NeuroImages software package (Cox 1996). Time series images were spatially registered in both 2- and 3-dimensional space to the second echo-planar image (EPI) of the first run to minimize effects of head motion, temporally interpolated to correct for slice-time acquisition differences, despiked, and blurred using a 3.5-mm full-width at half-maximum Gaussian kernel. A deconvolution analysis was then performed on a voxelwise basis to generate one hemodynamic response function (HRF) per condition. Participants' individual motion parameters were also entered as regressors of no interest in the model to reduce the impact of head motion on patterns of functional activation (Oakes et al. 2007). Each HRF was derived relative to the baseline state (visual fixation plus baseline gradient noise) and based on the first 16 s poststimulus onset. Functional images

were then interpolated to volumes with 1 mm^3 voxels, coregistered, and converted to a standard stereotaxic coordinate space (Talairach and Tournoux 1988). The images acquired 4.0–8.0 s poststimulus onset from the cue, corresponding to the peak of the HRF (Cohen 1997), were then averaged and divided by the model intercept to obtain an estimate of percent signal change (PSC).

A procedure that controlled for anatomical asymmetries through interhemispheric registration was also performed to facilitate direct voxelwise comparisons across the 2 hemispheres (Shulman et al. 2010). First, a raw EPI image from each subject was transformed to Talairach space. The resulting EPI image was then reflected around the anterior–posterior axis and registered to the nonreflected EPI image using a 12 degree-of-freedom affine transformation. The resulting transformation matrix from this procedure was then applied to the reflected PSC maps such that all right and left hemisphere data were registered into a single space.

The first set of analyses investigated the effects of stimulus presentation (i.e., lateralization) in either the right or the left hemifield. Specifically, two 2 × 2 (Laterality × Validity) repeated measures analyses of variance (ANOVAs) were performed on both behavioral and functional data to determine differential effects of laterality and cue validity (valid vs. invalid trials) during periods of facilitation (invalid RT > valid RT; 200 ms SOA) and IOR (valid RT > invalid RT; 700 ms SOA). Next, 4 voxelwise 2 × 2 (Hemisphere × Trial Laterality) repeated measures ANOVAs were also performed on the flipped and unflipped PSC data for valid and invalid trials at each SOA separately to directly investigate hemispheric asymmetries in evoked activation. A significance threshold corresponding to $P < 0.005$ was applied in combination with a minimum cluster size threshold of 832 µL (13 native voxels) to minimize false positives, which resulted in a corrected P value of 0.05 based on 10 000 Monte Carlo simulations (Forman et al. 1995).

To specifically examine activation in primary AC, T_1-weighted images were processed using the Freesurfer automated pipeline version 4.50 (Desikan et al. 2006), yielding subject-specific parcellations of the cerebral cortex based on individual gyral anatomy. From these parcellations, we obtained 2 regions of interest (ROIs) for primary AC corresponding to the right and left HGs (transverse temporal gyri), correcting them for any segmentation errors. While various imaging and histological studies restrict primary AC to the medial portion of HG (Abdul-Kareem and Sluming 2008), we chose to include the entire gyrus due to difficulties in determining this boundary using structural MRI alone.

Functional Connectivity Analyses
Identical preprocessing steps were followed with the resting-state scan. A regression analysis was then conducted on individual subjects' time series to remove potential sources of noise (physiological and machine-based) from the data based on established methodologies (Fox et al. 2005). Individual anatomical images (i.e., T_1) were first segmented into maps of white matter, gray matter, and cerebral spinal fluid (CSF), followed by calculation of an average time series for each tissue type. Next, the 6 movement parameters, the averaged time series for CSF and white matter, a constant term, and a linear term were entered into a linear regression against the extended resting-state time series. The residual time-series

data were then transformed into a standardized coordinate space (Talairach and Tournoux 1988). To facilitate voxelwise comparisons of intrinsic activity dependent on the placement of hemisphere seeds (see Supplementary Fig. 1), the time series data were reflected about the anterior–posterior axis (right to left hemisphere) and spatially registered (12 degree-of-freedom affine transformation).

Fifteen millimeter diameter spheres were used as seeds, located within the primary AC (39, –29, 10) or a more inferior secondary AC region (48, –26, –2) for both reflected and nonreflected data. Seed locations were generated based on clusters that exhibited left (primary AC) or right (secondary AC) hemisphere dominance in the hemisphere by trial laterality analyses of the auditory orienting task (see Results). Pearson's correlation coefficients from each seed were converted to signed z-scores using Fisher's method to maintain correlation directionality. Two 2 × 2 (Hemisphere × Seed Laterality) voxelwise repeated measures ANOVAs were performed separately on z-score volumes for the primary AC and secondary AC seeds.

Analyses of hemispheric asymmetries in intrinsic activity were restricted to ROI comprised of bilateral AC areas (insular cortex, temporal pole, superior and middle temporal gyrus [anterior and posterior divisions], HG, PT, planum polare, frontal, central, and parietal operculum) based on the Harvard–Oxford probabilistic atlas. A small volume correction (corrected $P < 0.05$) was then applied to the connectivity results ($P < 0.005$; 6 native voxels) based on the results from 10 000 Monte Carlo simulations (Forman et al. 1995).

Results

Behavioral Data

Behavioral results indicated a high overall accuracy rate (97.5%), demonstrating that participants had little difficulty performing the task. Two 2 × 2 (Laterality × Validity) repeated measures ANOVAs were performed on RT data for each SOA separately. Analyses of data for 200 ms SOA trials showed a main effect of laterality ($F_{1,26} = 10.11$, $P < 0.005$), with left target trials having faster RTs (mean = 550.9 ± 123.0 ms [SD]) than right target trials (mean = 583.9 ± 130.0 ms). The main effect of validity ($F_{1,26} = 10.17$, $P < 0.005$) was also significant, with faster RTs for valid (mean = 541.7 ± 112.7 ms) than invalid trials (mean = 593.1 ± 146.1 ms).

The 700 ms SOA results also indicated a main effect of laterality ($F_{1,26} = 10.14$, $P < 0.005$), with left target trials (mean = 478.9 ± 107.7 ms) responded to faster than right target trials (mean = 501.2 ± 112.8 ms). The main effect of validity was also significant ($F_{1,26} = 24.08$, $P < 0.001$), with faster RTs for invalid trials (mean = 465.5 ± 113.6 ms) than valid trials (mean = 514.6 ± 110.0 ms), indicating IOR. Interaction effects were not significant at either SOA.

Functional Data

Laterality and Validity Effects during Facilitation (200 ms SOA)

Two 2 × 2 (Laterality × Validity) repeated measures ANOVAs were performed separately for 200 (rapid/adaptive attentional state) and 700 ms (more static attentional state/IOR) SOA trials (Supplementary Table 1). The analysis of 200 ms SOA data indicated a laterality by validity interaction effect in the bilateral primary and secondary AC (Fig. 2A, left) and in the left fusiform gyrus. Simple effects paired t-tests on mean PSC within these clusters were performed to investigate the source of these interactions (Fig. 2B). For valid trials (i.e., both cues and targets in same hemifield), greater activity was observed in the AC for contralateral compared with ipsilateral stimuli in the group analyses, and this contralateral bias was fairly robust in individual subject analyses (left AC: 23/27 subjects [85%] showed pattern; right AC: 21/27 subjects [78%]). No differences in activation were found between invalid left and right trials.
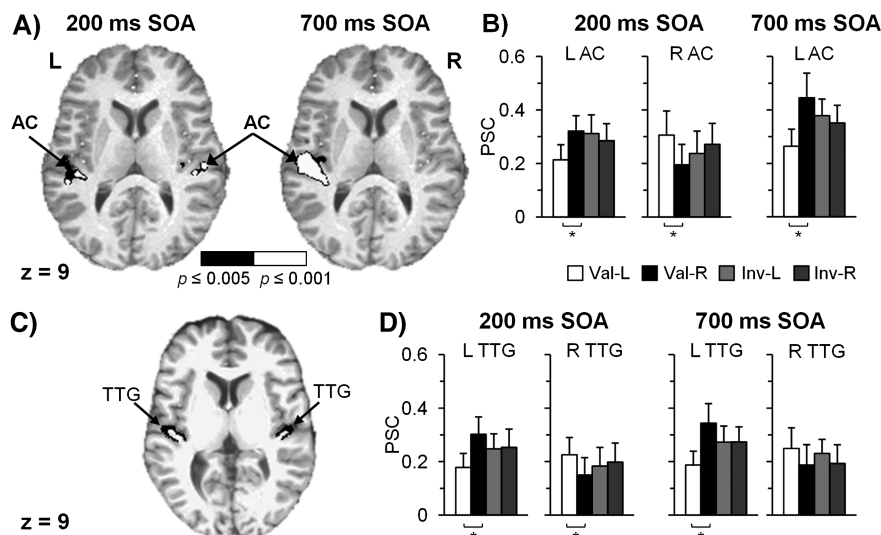

Figure 2. Panel A displays regions demonstrating Laterality × Validity interaction effects for 200 and 700 ms SOA in the left and right figures, respectively. Clusters of significant activation were present in the AC bilaterally at 200 ms SOA and in the left AC only at 700 ms SOA. Color scale indicates voxel-level significance (black, P < 0.005; white, P < 0.001). Panel B presents mean PSC for valid left (Val-L, white), valid right (Val-R, black), invalid left (Inv-L, light gray), and invalid right (Inv-R, dark gray) conditions for clusters within the AC. Panel C displays a sample of automatic parcellation (black areas) of the transverse temporal gyrus (TTG) in one subject, whereas Panel D presents mean group PSC within the TTG for the 4 trial conditions. Slices are located at 9 mm superior to the origin in Talairach space. All error bars represent 2 × standard error of the mean. Bracketed asterisks indicate significant findings (P < 0.05).

A main effect of validity (invalid trials > valid trials) was significant within areas of the frontoparietal reorienting network (Supplementary Fig. 2; Supplementary Table 2) including the presupplementary and supplementary motor area (pre-SMA/SMA), left inferior and superior parietal lobules extending into the precuneus, the bilateral superior temporal gyrus, and the bilateral anterior insulae. Greater activation for invalid trials was also observed in bilateral visual areas including the cuneus and lingual gyrus. A main effect of laterality was not observed in any regions, including the AC.

Laterality and Validity Effects during IOR (700 ms SOA)
A significant laterality by validity interaction effect (Fig. 2*A*; Supplementary Table 1) was present at the 700 ms SOA in the left primary and secondary AC extending into the insula. Simple effects analyses of the interaction effect (Fig. 2*B*) indicated greater contralateral activation for valid right compared with left trials in the left AC (26/27 subjects [96%] demonstrate contralateral bias) and no differences between invalid left and right trials. An interaction effect was also present in the bilateral cingulate gyrus, with follow-up *t*-tests also indicating greater activation for right-cued trials. A main effect of laterality (contralateral target trials > ipsilateral target trials) was also present within the left primary and secondary AC (Supplementary Table 3). The main effect of validity was not significant.

Analysis of Primary AC Data
The PSC for each of the conditions was also extracted and plotted separately for the primary AC only, based on an automatic parcellation scheme of T_1 images (Fig. 2*C*; Desikan et al. 2006). Results suggested a similar pattern of greater activation for contralaterally cued valid trials (Fig. 2*D*) bilaterally at the 200 ms SOA (left primary AC: $t_{26} = 3.72$, $P < 0.005$; right primary AC: $t_{26} = 2.44$, $P < 0.05$) and in the left hemisphere at 700 ms SOA ($t_{26} = 5.48$, $P < 0.001$). This effect reached only a trend level of significance for the right hemisphere at the 700 ms SOA ($P = 0.062$), suggesting a slight reduction in contralateral bias. There were no differences in PSC for invalidly cued trials within the primary AC.

Direct Voxelwise Comparisons of Hemispheric Asymmetries
The next series of analyses directly compared activation in the right and left hemispheres as a function of cue validity and laterality. This was achieved by reflecting the fMRI data around the *y*-axis and registering the reflected and nonreflected data together for each subject. Four 2 × 2 (Hemisphere × Laterality) repeated measures ANOVAs were conducted separately for each of the 4 primary conditions (valid and invalid trials at the 200 and 700 ms SOA) across the entire group. A main effect of hemisphere in this analytic framework indicates regions demonstrating asymmetric activation regardless of stimulus location in extrapersonal space (i.e., for trials in both left and right hemifields). A main effect of laterality suggests that symmetric areas in both hemispheres demonstrated differential activation for stimuli in one hemifield. Results are reported using Talairach coordinates of clusters in the left hemisphere only, as activation in the right hemisphere should be symmetric but inverse in sign following the transformation and registration (Shulman et al. 2010).

A hemisphere by laterality interaction was observed for validly cued trials at both the 200 and 700 ms SOA in a large cluster within the primary and anterior secondary AC (Fig. 3; Supplementary Table 4). Simple effects *t*-tests indicated an
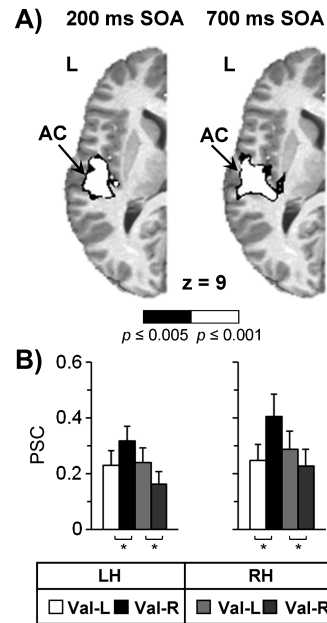

Figure 3. Auditory regions (Panel A) that demonstrated a Hemisphere × Laterality interaction effect at 200 and 700 ms SOA. Color scale indicates voxel-level significance (black, P < 0.005; white, P < 0.001). Panel B presents mean PSC for valid left (Val-L) or valid right (Val-R) trials in left hemisphere (LH; white or black, respectively) and valid left or valid right in right hemisphere (RH; light gray and dark gray, respectively). Slices are located at 9 mm superior to the origin in Talairach space. All error bars represent 2 × standard error of the mean. Bracketed asterisks indicate significant findings (P < 0.05).

overall pattern of greater activation for contralateral stimuli bilaterally at both SOAs. This effect was robust across individual subjects at the 200 ms SOA (19/27 subjects [70%] showed contralateral bias in the left AC; 21/27 subjects (78%) in the right AC), but became relatively more pronounced for the left AC compared with the right AC at the 700 ms SOA (left AC: 25/27 subjects [93%]; right AC: 18/27 subjects [67%]). A contralaterality index (CI; contralateral–ipsilateral stimulus activation) was computed to further quantify differences in contralateral bias between left and right AC (i.e., neglect theory). Results indicated that the left (CI = 0.09 ± 0.13) and right (CI = 0.08 ± 0.12) AC demonstrated similar degrees of contralateral bias at 200 ms SOA ($P > 0.10$). In contrast, at 700 ms SOA, the left AC (CI = 0.16 ± 0.13) demonstrated greater contralateral bias compared with the right AC (CI = 0.06 ± 0.12; $t_{26} = 2.10$. $P < 0.05$), which primarily resulted from increased bias in the left AC relative to the 200 ms trials (see Fig. 3*B*).

Results indicated that a similar pattern of hemispheric asymmetries was observed across all 4 ANOVAs, suggestive of 2 large-scale networks, one involved in spatial attention and the other in task-related motor responses (Fig. 4; Supplementary Table 5). Greater activation of the posterior parietal lobes and temporoparietal junction and the posterior cingulate cortex/precuneus was observed within the right compared with the left hemisphere across all 4 ANOVAs. In addition, several frontal regions including the dorsal anterior cingulate cortex (ACC)/pre-SMA and dorsolateral prefrontal cortex demonstrated a strong right hemisphere bias across 3 of the 4 ANOVAs. Task-related right-handed motor responses accounted for greater activation in the right cerebellum, left pre-SMA/SMA, and left sensorimotor cortex. Greater left hemisphere activity was also observed in the thalamus.

In addition, a striking segregation of the AC was achieved. The primary AC exhibited greater left hemisphere activation across all 4 ANOVAs. In contrast, greater right hemisphere activation was observed within an area of the secondary AC in the PT, extending into an area of the superior temporal gyrus located inferior to the area of greater left hemisphere activation. This region of right hemisphere dominance in the PT did not exhibit spatial overlap with any of the effects observed in the laterality by validity analyses.

fcMRI Analyses of Intrinsic Activity

A series of 2 × 2 (Hemisphere × Seed laterality) ANOVAs were used to examine hemispheric asymmetries in intrinsic activity as a function of hemisphere (i.e., ipsilateral or contralateral to seed location) and seed placement (in right or left hemisphere; see Supplementary Fig. 1). This allows comparison of connectivity both within hemisphere (e.g., left seed and left hemisphere [S_LH_L]) and between hemispheres (e.g., right seed and left hemisphere [S_RH_L]).

Resting-state data were residualized for known noise sources based on established methodologies (Fox et al. 2005), and primary versus secondary AC seeds were obtained based on the empirical results from regions demonstrating hemispheric asymmetries in evoked activity (Fig. 5A). In this analytic framework, the interaction term indicated hemispheric (right vs. left) differences in either ipsilateral or contralateral connectivity. A main effect of hemisphere (ipsilateral > contralateral)
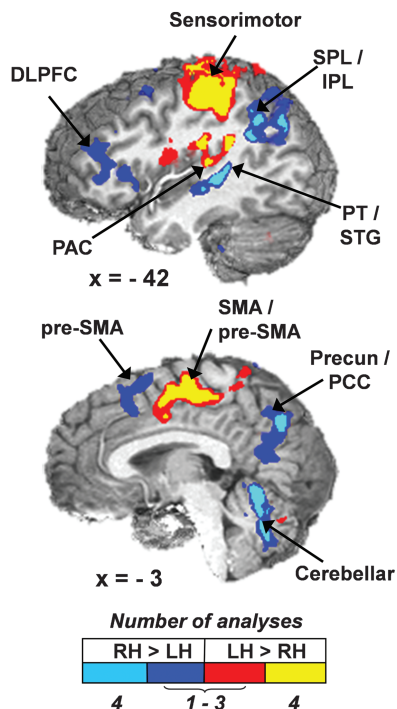
was expected within seed regions and beyond as correlations should be higher within the seeded hemisphere compared with the contralateral hemisphere. A main effect of seed laterality indicated whether the left or right seed has greater correlation with symmetric homologous areas in both hemispheres.

Results from the fcMRI analyses of the primary AC seed are presented first (Fig. 5B,C, left column; Table 1). A significant interaction term was observed within the primary AC, with simple effects tests indicating higher ipsilateral connectivity for
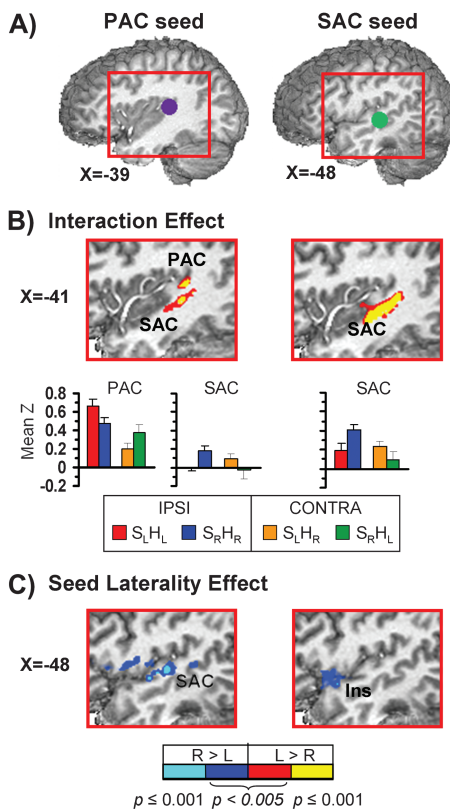

Figure 5. This figure presents regions that exhibited differences in intrinsic activity based on seed placement (Panel A) in the primary (PAC, purple seed) versus secondary (SAC, green seed) AC. Panel B presents hemisphere × seed laterality interaction effects for PAC (left column) and SAC (right column) seed. Bar graphs represent mean z-scores (error bars = 2 × standard error of the mean) for each of the 4 conditions (red, S_LH_L; blue, S_RH_R; orange, S_LH_R; green, S_RH_L) within clusters in the PAC, SAC and insula (Ins). Panel C presents main effects of seed laterality for PAC seed analyses (left column) and SAC seed analyses (right column). Regions that exhibited higher connectivity with the right seed (S_R) are presented in cool colors, whereas regions that exhibited higher connectivity with the left seed (S_L) are presented in warm colors. Color scale indicates voxel-level significance (dark blue and red, P < 0.005; cyan and yellow, P ≤ 0.001). Slices are located at x = −39 (PAC seed), x = −48 (SAC seed and Panel C) or x = −41 mm (Panel B) to the left of the origin in Talairach space.

Figure 4. Hemispheric asymmetries in functional activation. Greater right (RH) compared with left (LH) hemisphere activation (cool colors) was observed in dorsolateral prefrontal cortex (DLPFC), superior and inferior parietal area (SPL/IPL), PT and superior temporal gyrus (STG), pre-SMA, precuneus and posterior cingulate cortex (Precun/PCC), and cerebellar areas. Greater left compared with right hemisphere activation (warm colors) was observed in the sensorimotor areas, primary auditory cortex (PAC), and SMA/pre-SMA. Color scale indicates the number of analyses with overlapping areas of significant activation (dark blue and red, 1–3 trial conditions; cyan and yellow, all 4 trial conditions) Slices are located at x = −42 or −3 mm to the left of the origin in Talairach space.

Table 1

Results of interaction term from functional connectivity analyses

Region	x	y	z	Volume (mL)	Ipsilateral	Contralateral
Primary AC seed						
Primary AC	−39	−32	10	0.480	$S_LH_L > S_RH_R$	$S_RH_L > S_LH_R$
Secondary AC	−40	−29	−1	0.495	$S_RH_R > S_LH_L$	$S_LH_R > S_RH_L$
Secondary AC Seed						
Secondary AC	−41	−28	0	1.625	$S_RH_R > S_LH_L$	$S_LH_R > S_RH_L$

Note: The center of mass in Talairach coordinates (x, y, z) and the volume in milliliters (mL) are specified for each area of activation. Results from simple effects testing are presented for the hemispheres ipsilateral (within hemisphere connectivity) and contralateral (across hemisphere connectivity) to seed placement. S_XH_Y = connectivity between X seed and Y hemisphere, where S_L = left seed, S_R = right seed, H_L = left hemisphere, H_R = right hemisphere.

the left relative to right primary AC seed (t_{26} = 5.46, P < 0.001), as well as higher contralateral (i.e., between hemisphere) connectivity for the right compared with left seed (t_{26} = –5.78, P < 0.001). This constellation of interaction effects was also observed at the individual subject level (S_LH_L > S_RH_R in primary AC in 77.8% of subjects; S_RH_L > S_LH_R in 85.1% of subjects) and suggests greater connectivity in the left primary AC regardless of seed placement. A significant interaction term was also observed within the secondary AC, although the pattern of ipsilateral (right seed > left seed; [t_{26} = –5.63, P < 0.001]) and contralateral connectivity (left seed > right seed; [t_{26} = 4.06, P < 0.001]) was now reversed. This pattern was also reversed at the individual level in a majority of subjects (S_RH_R > S_LH_L = 81.5%; S_LH_R > S_RH_L = 85.1%). Significant main effect of seed laterality indicated greater connectivity between the right primary AC seed and the bilateral areas of the secondary AC, insula, precentral gyrus, and inferior frontal gyrus compared with the left primary AC seed.

When the seeds were placed in secondary AC, a significant interaction term was observed within the secondary AC (SAC; Fig. 5B, right column; Table 1), with greater right ipsilateral (S_RH_R > S_LH_L in 96.3% of subjects; t_{26} = –7.54, P < 0.001) and left contralateral (S_LH_R > S_RH_L in 88.9% of subjects; t_{26} = 6.20, P < 0.001) connectivity. A main effect of seed laterality indicated greater connectivity within the anterior insula and superior temporal gyrus for the right relative to left seed (Fig. 5C, right column).

In addition, several supplementary analyses were conducted to minimize the contribution of morphological asymmetries between the right and the left hemisphere in our functional connectivity analyses. Specifically, we examined the effects of using the high-resolution anatomical (T_1) rather than EPI images (higher resolution and contrast) to derive the cross-hemisphere registration matrix. We also controlled for hemispheric differences in gray matter volume within the primary and secondary AC spheres. However, similar to our original analyses, the observed asymmetries in functional connectivity remained present within the AC in both of the supplemental analyses.

Discussion

Current results are consistent with previous studies of auditory and visual spatial attention (Posner and Cohen 1984; Rafal et al. 1989; Lepsien and Pollmann 2002; Mayer et al. 2004; Mayer et al. 2007), confirming successful induction of exogenous orienting. Specifically, RT is slower following reorienting of attention during invalid compared with valid trials (facilitation) at 200 ms SOA, whereas RT is faster for invalid trials (IOR) at 700 ms SOA. Likewise, functional results confirmed the involvement of a lateral prefrontal and posterior parietal network in attentional reorienting (invalid > valid activation) at short SOAs (Arrington et al. 2000; Vandenberghe et al. 2001; Corbetta and Shulman 2002; Mayer et al. 2007), with no difference across validly and invalidly cued trials during IOR. Greater activity for invalid compared with valid trials was also observed in the bilateral AC at 200 ms SOA. Invalid trials differ from valid trials not only in cueing validity but also in stimulus location. As previous studies (Ahveninen et al. 2006; Altmann et al. 2007) have reported greater activation for the second of a pair of stimuli when it occurs at a different location than the first stimulus, increased activation in the AC during invalid cues

may be secondary to attentional effects (reorienting) or a result of the change in stimulus location.

Our behavioral results were consistent with previous reports (Krumbholz et al. 2009) indicating a lateralization effect, with RTs significantly faster for trials presented in the left hemifield regardless of cue validity or SOA. Kimura et al. (Kimura 1961; Hugdahl et al. 2008) have theorized that the spatial proximity of left AC to left hemisphere language centers promotes more efficient language processing, resulting in a right-ear advantage during dichotic presentations. Likewise, the bias toward left hemifield trials may be the result of the proximity of the right AC to the right hemisphere–dominant spatial attention network. Current results provide some support for this hypothesis, as greater functional activation was observed in right dorsal ACC/pre-SMA and lateral frontoparietal regions across the majority of trial types, irrespective of stimulus location, validity, or SOA.

These lateral frontoparietal areas likely serve as the supramodal representation of extrapersonal visual (Santangelo et al. 2009; Shulman et al. 2010) and auditory (Zatorre et al. 1999; Lewald et al. 2008) space and provide additional evidence for clinical observations of hemispatial neglect more frequently following right compared with left hemisphere lesions (Bellmann et al. 2001; Spierer et al. 2009; Gainotti 2010). Moreover, a similar frontoparietal network has also been implicated in adjusting attentional control (Dosenbach et al. 2007), which frequently occurs during a cueing paradigm. However, previous studies of auditory spatial attention utilizing voxelwise interhemispheric comparisons have produced mixed evidence for right frontoparietal dominance (Mayer et al. 2006; Petit et al. 2007; Krumbholz et al. 2009), suggesting that discrepancies in task stimuli (verbal vs. nonverbal; Krumbholz et al. 2009) and nature of attentional allocation (voluntary vs. automatic; Kim et al. 1999; Mayer et al. 2006) may interact with these hemispheric asymmetries.

In contrast to right-lateralized frontoparietal findings, hemispheric asymmetries within the AC were divided between the 2 hemispheres according to primary versus secondary regions (Petit et al. 2007), with the left primary AC and right PT consistently demonstrating dominance across all trial types. The left primary AC likely serves as the initial basic sound processing center (Devlin et al. 2003; Petit et al. 2007), where temporal and spectral complexity of incoming stimuli are triaged, before being further processed either by left hemisphere language areas or by right AC for more complex spectral properties (Zatorre and Belin 2001; Petit et al. 2007; Okamoto et al. 2009). However, the relatively basic spectral properties of our stimuli (pure tones) may not have required additional right hemisphere processing, suggesting that the spatial nature of the orienting task resulted in greater activation within the right PT.

Support for this hypothesis can be derived from primate (Kaas and Hackett 2000; Rauschecker and Tian 2000) and human (Weeks et al. 1999; Langers et al. 2007) studies indicating that the "what" and "where" streams of auditory processing diverge between primary and secondary AC, with spatial processing mainly occurring within posterior supratemporal regions (Spierer et al. 2009). The posterior superior temporal gyrus also projects to frontal and parietal regions implicated in spatial attention (Romanski et al. 1999) and exhibits greater right hemisphere activity during visual target detection (Shulman et al. 2010). Thus, the right hemisphere dominance of the posterior superior temporal gyrus in the context of the current and previous studies suggests that this structure is also critical for auditory localization, and along with

the right lateral frontoparietal network, may form a supramodal network for monitoring extrapersonal space (where stream). In contrast, the left primary AC may be the hub of the what stream, evaluating basic properties of incoming auditory stimuli before forwarding to other cortical structures for more complex processing.

Intriguingly, current results provide the first evidence that specialization of function across hemispheres may extend its influence during spontaneous neuronal activity within the AC. A previous study (Liu et al. 2009) examining laterality effects in intrinsic fluctuations indicated left dominance in language and default-mode areas, coupled with right dominance in visual areas and in regions implicated in the detection of unattended events (angular gyrus and insula). Current results indicate that functional connectivity was greater in the left primary AC for both left and right hemisphere primary AC seed placements, suggesting a more synchronized pattern of neuronal activity in the task-dominant region regardless of external demands (Supplementary Fig. 3A). Similarly, intrinsic activity in secondary AC (PT) was more synchronized in the right hemisphere for both primary and secondary AC seed placements (Supplementary Fig. 3B,C).

Intrinsic activity may serve as a record of previous task-dependent usage, may coordinate neuronal activity between regions that are traditionally coactivated, or may represent a dynamic prediction of future use (Fox and Raichle 2007). Thus, the relatively larger evoked responses observed in left primary AC (i.e., basic stimulus processing; Devlin et al. 2003; Petit et al. 2007) and right PT (i.e., spatial processes; Spierer et al. 2009; Shulman et al. 2010) during auditory orienting may be reflective of both task-related modulations and an inherent dominance in the synchronization of intrinsic activity. However, previous studies have also reported hemispheric asymmetries in the spatial location and volume of both white and gray matter structures in the AC (Penhune et al. 1996; Toga and Thompson 2003; Van Essen 2005). Therefore, although several supplemental analyses were conducted to minimize the contribution of structural asymmetries to our intrinsic activity, the contribution of morphometric differences cannot be fully excluded. Moreover, future studies should examine differences in hemispheric asymmetries during intrinsic activity in other regions of the brain outside of the AC.

A primary aim of the current study was to investigate models of contralateral bias (Alho et al. 1999; Richter et al. 2009; Woods et al. 2009) and neglect (Deouell et al. 1998; Kaiser et al. 2000; Krumbholz et al. 2007) in terms of AC functioning during auditory spatial localization. Functional results indicated that evidence for each model was strongly dependent on the interval between cue and target, and thus the attentional states that were induced. During facilitated (i.e., rapid/adaptive) orienting of attention (200 ms SOA), strong evidence for the contralateral bias theory emerged for both the left and the right AC on group and individual subject levels. Subject-specific ROI analyses also confirmed that the contralateral bias existed within the left and right primary AC as well as secondary cortical areas.

In contrast, support for the neglect model was more prominent during IOR, evoked by a longer duration between cue and target. Specifically, significant effects of laterality (main effect or interaction) were not present within the right AC (700 ms SOA), whereas a greater percentage of subjects (96%) demonstrated contralateral bias within the left AC at the 700 ms relative to 200 ms SOA. In addition, when activity across the 2 hemispheres was directly contrasted (voxelwise analyses), the percentage of subjects demonstrating contralateral bias increased (70-93%) for the left and slightly decreased (78-67%) for the right AC from the 200 to 700 ms SOA. Finally, a significant difference (left AC > right AC) in an index of contralaterality bias was only present at the 700 ms SOA; however, this appeared to result from increased bias for right stimuli in the left AC. In summary, these results provide strong evidence of increasing contralateral bias in the left AC in conjunction with moderate evidence of decreasing contralateral bias in the right AC during the IOR at longer cue–target intervals. This constellation of findings is consistent with the neglect model (Fig. 1), which predicts that the right hemisphere allocates attention to both hemifields, whereas the left hemisphere is strongly biased to right hemifield stimuli (Bartolomeo and Chokron 2002; Corbetta et al. 2005).

Absent attentional modulation through higher-order cortical structures, animal studies (Moore et al. 1984; Irvine 1986) suggest that a contralateral bias would be the expected default model of functioning. Specifically, approximately 25% of the neurons in the inferior colliculus are monaural, responding only to the contralateral ear (EO neurons), while the other 75% are binaural, among which 30–40% receive excitatory input from the contralateral ear and inhibitory input from the ipsilateral ear (EI neurons). The remainder receives excitatory input from both ears (EE neurons; Rouiller 1997). Thus, the auditory pathway may be hardwired for a contralaterally biased response, and deviations from this default pattern are likely modulated by higher level attentional networks such as the right lateral frontoparietal cortex. The native contralateral bias in the right AC may be inhibited by right-lateralized spatial networks during more prolonged attentional states such that focus is more globally and diffusely distributed across both hemifields.

In summary, current findings suggest that the contralateral and neglect models of spatial processing within AC areas are not mutually exclusive. Contralateral bias may be modulated by attentional context and present for both hemispheres during the automatic orienting of attention, then gradually increase within the left AC and decrease within the right AC as automatic attentional capture subsides. The induction of IOR occurs with the passage of time, putatively influenced by the right hemisphere dominant attention network. However, previous studies (Belin et al. 1998; Zatorre et al. 2002; Brunetti et al. 2008; Salminen et al. 2010) indicate that patterns of auditory activation are influenced by stimulus types (complex spectra, white noise, linguistic or other sounds recorded from nature, etc.) and mode of presentation (binaural, free-field head-related transfer function), such that current results require additional study.

Current findings also suggest left hemisphere dominance in primary AC for the processing of sounds and right hemisphere dominance in PT for processing of spatial information. Perhaps most interestingly, our fcMRI analyses provide provocative evidence that these hemispheric asymmetries in the AC are also present during intrinsic neuronal activity. While speculative, these findings provide preliminary evidence that intrinsic neuronal activity in the task-dominant hemisphere may be more synchronized than activity in the nondominant hemisphere.

Supplementary Material

Supplementary material can be found at: http://www.cercor.oxfordjournals.org/

References

Abdul-Kareem IA, Sluming V. 2008. Heschl gyrus and its included primary auditory cortex: structural MRI studies in healthy and diseased subjects. J Magn Reson Imaging. 28:287–299.

Ahveninen J, Jaaskelainen IP, Raij T, Bonmassar G, Devore S, Hamalainen M, Levanen S, Lin FH, Sams M, Shinn-Cunningham BG, et al. 2006. Task-modulated "what" and "where" pathways in human auditory cortex. Proc Natl Acad Sci U S A. 103:14608–14613.

Alho K, Medvedev SV, Pakhomov SV, Roudas MS, Tervaniemi M, Reinikainen K, Zeffiro T, Naatanen R. 1999. Selective tuning of the left and right auditory cortices during spatially directed attention. Brain Res Cogn Brain Res. 7:335–341.

Altmann CF, Bledowski C, Wibral M, Kaiser J. 2007. Processing of location and pattern changes of natural sounds in the human auditory cortex. Neuroimage. 35:1192–1200.

Arrington CM, Carr TH, Mayer AR, Rao SM. 2000. Neural mechanisms of visual attention: object-based selection of a region in space. J Cogn Neurosci. 12:106–117.

Bartolomeo P, Chokron S. 2002. Orienting of attention in left unilateral neglect. Neurosci Biobehav Rev. 26:217–234.

Belin P, McAdams S, Smith B, Savel S, Thivard L, Samson S, Samson Y. 1998. The functional anatomy of sound intensity discrimination. J Neurosci. 18:6388–6394.

Bellmann A, Meuli R, Clarke S. 2001. Two types of auditory neglect. Brain. 124:676–687.

Brunetti M, Della PS, Ferretti A, Del GC, Cianflone F, Belardinelli P, Caulo M, Pizzella V, Olivetti BM, Romani GL. 2008. A frontoparietal network for spatial attention reorienting in the auditory domain: a human fMRI/MEG study of functional and temporal dynamics. Cereb Cortex. 18:1139–1147.

Burock MA, Buckner RL, Woldorff MG, Rosen BR, Dale AM. 1998. Randomized event-related experimental designs allow for extremely rapid presentation rates using functional MRI. Neuroreport. 9:3735–3739.

Cohen M. 1997. Parametric analysis of fMRI data using linear systems methods. Neuroimage. 6:93–103.

Corbetta M, Shulman GL. 2002. Control of goal-directed and stimulus-driven attention in the brain. Nat Rev Neurosci. 3:201–215.

Corbetta M, Kincade MJ, Lewis C, Snyder AZ, Sapir A. 2005. Neural basis and recovery of spatial attention deficits in spatial neglect. Nat Neurosci. 8:1603–1610.

Corbetta M, Kincade JM, Ollinger JM, McAvoy MP, Shulman GL. 2000. Voluntary orienting is dissociated from target detection in human posterior parietal cortex. Nat Neurosci. 3:292–297.

Cox RW. 1996. AFNI: software for analysis and visualization of functional magnetic resonance neuroimages. Comput Biomed Research. 29:162–173.

Deouell LY, Bentin S, Giard MH. 1998. Mismatch negativity in dichotic listening: evidence for interhemispheric differences and multiple generators. Psychophysiology. 35:355–365.

Desikan RS, Segonne F, Fischl B, Quinn BT, Dickerson BC, Blacker D, Buckner RL, Dale AM, Maguire RP, Hyman BT, et al. 2006. An automated labeling system for subdividing the human cerebral cortex on MRI scans into gyral based regions of interest. Neuroimage. 31:968–980.

Devlin JT, Raley J, Tunbridge E, Lanary K, Floyer-Lea A, Narain C, Cohen I, Behrens T, Jezzard P, Matthews PM, et al. 2003. Functional asymmetry for auditory processing in human primary auditory cortex. J Neurosci. 23:11516–11522.

Dorsaint-Pierre R, Penhune VB, Watkins KE, Neelin P, Lerch JP, Bouffard M, Zatorre RJ. 2006. Asymmetries of the planum temporale and Heschl's gyrus: relationship to language lateralization. Brain. 129:1164–1176.

Dosenbach NU, Fair DA, Miezin FM, Cohen AL, Wenger KK, Dosenbach RA, Fox MD, Snyder AZ, Vincent JL, Raichle ME, et al. 2007. Distinct brain networks for adaptive and stable task control in humans. Proc Natl Acad Sci U S A. 104:11073–11078.

Forman SD, Cohen JD, Fitzgerald M, Eddy WF, Mintun MA, Noll DC. 1995. Improved assessment of significant activation in functional magnetic resonance imaging (fMRI): use of a cluster-size threshold. Magn Reson Med. 33:636–647.

Fox MD, Raichle ME. 2007. Spontaneous fluctuations in brain activity observed with functional magnetic resonance imaging. Nat Rev Neurosci. 8:700–711.

Fox MD, Snyder AZ, Vincent JL, Corbetta M, Van E, Raichle ME. 2005. The human brain is intrinsically organized into dynamic, anti-correlated functional networks. Proc Natl Acad Sci U S A. 102:9673–9678.

Gainotti G. 2010. The role of automatic orienting of attention towards ipsilesional stimuli in non-visual (tactile and auditory) neglect: a critical review. Cortex. 46:150–160.

Gilmore CS, Clementz BA, Berg P. 2009. Hemispheric differences in auditory oddball responses during monaural versus binaural stimulation. Int J Psychophysiol. 73:326–333.

Glover GH. 1999. Deconvolution of impulse response in event-related BOLD fMRI. Neuroimage. 9:416–429.

Hine J, Debener S. 2007. Late auditory evoked potentials asymmetry revisited. Clin Neurophysiol. 118:1274–1285.

Hugdahl K, Westerhausen R, Alho K, Medvedev S, Hamalainen H. 2008. The effect of stimulus intensity on the right ear advantage in dichotic listening. Neurosci Lett. 431:90–94.

Irvine DRF. 1986. A review of the structure and function of auditory brainstem processing mechanisms. In: Ottoson D, editor. Sensory physiology. Berlin (Germany): Springer Verlag. p. 1–279.

Kaas JH, Hackett TA. 2000. Subdivisions of auditory cortex and processing streams in primates. Proc Natl Acad Sci U S A. 97:11793–11799.

Kaiser J, Lutzenberger W, Preissl H, Ackermann H, Birbaumer N. 2000. Right-hemisphere dominance for the processing of sound-source lateralization. J Neurosci. 20:6631–6639.

Kim YH, Gitelman DR, Nobre AC, Parrish TB, LaBar KS, Mesulam MM. 1999. The large-scale neural network for spatial attention displays multifunctional overlap but differential asymmetry. Neuroimage. 9:269–277.

Kimura D. 1961. Some effects of temporal-lobe damage on auditory perception. Can J Psychol. 15:156–165.

Krumbholz K, Hewson-Stoate N, Schonwiesner M. 2007. Cortical response to auditory motion suggests an asymmetry in the reliance on inter-hemispheric connections between the left and right auditory cortices. J Neurophysiol. 97:1649–1655.

Krumbholz K, Nobis EA, Weatheritt RJ, Fink GR. 2009. Executive control of spatial attention shifts in the auditory compared to the visual modality. Hum Brain Mapp. 30:1457–1469.

Langers DR, Backes WH, van DP. 2007. Representation of lateralization and tonotopy in primary versus secondary human auditory cortex. Neuroimage. 34:264–273.

Lepsien J, Pollmann S. 2002. Covert reorienting and inhibition of return: an event-related fMRI study. J Cogn Neurosci. 14:127–144.

Lewald J, Riederer KA, Lentz T, Meister IG. 2008. Processing of sound location in human cortex. Eur J Neurosci. 27:1261–1270.

Liu H, Stufflebeam SM, Sepulcre J, Hedden T, Buckner RL. 2009. Evidence from intrinsic activity that asymmetry of the human brain is controlled by multiple factors. Proc Natl Acad Sci U S A. 106:20499–20503.

Mangun GR, Luck SJ, Plager R, Loftus W. 1994. Monitoring the visual world: hemispheric asymmetries and subcortical processes in attention. J Cogn Neurosci. 6:267–275.

Mayer AR, Harrington D, Adair JC, Lee R. 2006. The neural networks underlying endogenous auditory covert orienting and reorienting. Neuroimage. 30:938-949.

Mayer AR, Harrington DL, Stephen J, Adair JC, Lee RR. 2007. An event-related fMRI study of exogenous facilitation and inhibition of return in the auditory modality. J Cogn Neurosci. 19:455-467.

Mayer AR, Seidenberg M, Dorflinger JM, Rao SM. 2004. An event-related fMRI study of exogenous orienting: supporting evidence for the cortical basis of inhibition of return? J Cogn Neurosci. 16:1262-1271.

Mesulam MM. 1999. Spatial attention and neglect: parietal, frontal and cingulate contributions to the mental representation and attentional targeting of salient extrapersonal events. Philos Trans R Soc Lond B Biol Sci. 354:1325-1346.

Moore DR, Semple MN, Addison PD, Aitkin LM. 1984. Properties of spatial receptive fields in the central nucleus of the cat inferior colliculus. I. Responses to tones of low intensity. Hear Res. 13:159-174.

Oakes TR, Fox AS, Johnstone T, Chung MK, Kalin N, Davidson RJ. 2007. Integrating VBM into the General Linear Model with voxelwise anatomical covariates. Neuroimage. 34:500-508.

Okamoto H, Stracke H, Draganova R, Pantev C. 2009. Hemispheric asymmetry of auditory evoked fields elicited by spectral versus temporal stimulus change. Cereb Cortex. 19:2290-2297.

Oldfield RC. 1971. The assessment and analysis of handedness: the Edinburgh inventory. Neuropsychologia. 9:97-113.

Penhune VB, Zatorre RJ, MacDonald JD, Evans AC. 1996. Interhemispheric anatomical differences in human primary auditory cortex: probabilistic mapping and volume measurement from magnetic resonance scans. Cereb Cortex. 6:661-672.

Petit L, Simon G, Joliot M, Andersson F, Bertin T, Zago L, Mellet E, Tzourio-Mazoyer N. 2007. Right hemisphere dominance for auditory attention and its modulation by eye position: an event related fMRI study. Restor Neurol Neurosci. 25:211-225.

Posner MI, Cohen Y. 1984. Components of visual orienting. In: Bouma H, Bowhuis D, editors. Attention and performance. London: Lawrence Erlbaum. p. 531-556.

Rademacher J, Morosan P, Schormann T, Schleicher A, Werner C, Freund HJ, Zilles K. 2001. Probabilistic mapping and volume measurement of human primary auditory cortex. Neuroimage. 13:669-683.

Rafal RD, Calabresi PA, Brennan CW, Sciolto TK, Posner MI, Walker JA, Friedrich FA, Rafal RD, Posner MI, Rafal RD, et al. 1989. Saccade preparation inhibits reorienting to recently attended locations. J Exp Psychol Hum Percept Perform. 15:673-685.

Raichle ME, Mintun MA. 2006. Brain work and brain imaging. Annu Rev Neurosci. 29:449-476.

Rauschecker JP, Tian B. 2000. Mechanisms and streams for processing of "what" and "where" in auditory cortex. Proc Natl Acad Sci U S A. 97:11800-11806.

Richter N, Schroger E, Rubsamen R. 2009. Hemispheric specialization during discrimination of sound sources reflected by MMN. Neuropsychologia. 47:2652-2659.

Romanski LM, Bates JF, Goldman-Rakic PS. 1999. Auditory belt and parabelt projections to the prefrontal cortex in the rhesus monkey. J Comp Neurol. 403:141-157.

Rouiller EM. 1997. Functional organization of auditory pathways. In: Ehret G, Romand R, editors. The central auditory system. New York: Oxford University Press. p. 3-96.

Salminen NH, Tiitinen H, Miettinen I, Alku P, May PJ. 2010. Asymmetrical representation of auditory space in human cortex. Brain Res. 1306:93-99.

Santangelo V, Olivetti BM, Spence C, Macaluso E. 2009. Interactions between voluntary and stimulus-driven spatial attention mechanisms across sensory modalities. J Cogn Neurosci. 21:2384-2397.

Schonwiesner M, Krumbholz K, Rubsamen R, Fink GR, von Cramon DY. 2007. Hemispheric asymmetry for auditory processing in the human auditory brain stem, thalamus, and cortex. Cereb Cortex. 17:492-499.

Shulman GL, Pope DL, Astafiev SV, McAvoy MP, Snyder AZ, Corbetta M. 2010. Right hemisphere dominance during spatial selective attention and target detection occurs outside the dorsal frontoparietal network. J Neurosci. 30:3640-3651.

Smith SM, Fox PT, Miller KL, Glahn DC, Fox PM, Mackay CE, Filippini N, Watkins KE, Toro R, Laird AR, et al. 2009. Correspondence of the brain's functional architecture during activation and rest. Proc Natl Acad Sci U S A. 106:13040-13045.

Spierer L, Bellmann-Thiran A, Maeder P, Murray MM, Clarke S. 2009. Hemispheric competence for auditory spatial representation. Brain. 132:1953-1966.

Talairach J, Tournoux P. 1988. Co-planar steriotaxic atlas of the human brain. New York: Thieme.

Tanaka H, Hachisuka K, Ogata H. 1999. Sound lateralisation in patients with left or right cerebral hemispheric lesions: relation with unilateral visuospatial neglect. J Neurol Neurosurg Psychiatry. 67:481-486.

Toga AW, Thompson PM. 2003. Mapping brain asymmetry. Nat Rev Neurosci. 4:37-48.

Van Essen DC. 2005. A population-average, landmark- and surface-based (PALS) atlas of human cerebral cortex. Neuroimage. 28:635-662.

Vandenberghe R, Gitelman DR, Parrish TB, Mesulam MM. 2001. Location- or feature-based targeting of peripheral attention. Neuroimage. 14:37-47.

Weeks RA, Aziz-Sultan A, Bushara KO, Tian B, Wessinger CM, Dang N, Rauschecker JP, Hallett M. 1999. A PET study of human auditory spatial processing. Neurosci Lett. 262:155-158.

Westbury CF, Zatorre RJ, Evans AC. 1999. Quantifying variability in the planum temporale: a probability map. Cereb Cortex. 9:392-405.

Woldorff MG, Tempelmann C, Fell J, Tegeler C, Gaschler-Markefski B, Hinrichs H, Heinz HJ, Scheich H. 1999. Lateralized auditory spatial perception and the contralaterality of cortical processing as studied with functional magnetic resonance imaging and magnetoencephalography. Hum Brain Mapp. 7:49-66.

Woods DL, Stecker GC, Rinne T, Herron TJ, Cate AD, Yund EW, Liao I, Kang X. 2009. Functional maps of human auditory cortex: effects of acoustic features and attention. PLoS One. 4:e5183.

Zatorre RJ, Belin P. 2001. Spectral and temporal processing in human auditory cortex. Cereb Cortex. 11:946-953.

Zatorre RJ, Bouffard M, Ahad P, Belin P. 2002. Where is 'where' in the human auditory cortex? Nat Neurosci. 5:905-909.

Zatorre RJ, Mondor TA, Evans AC. 1999. Auditory attention to space and frequency activates similar cerebral systems. Neuroimage. 10:544-554.

Zatorre RJ, Penhune VB. 2001. Spatial localization after excision of human auditory cortex. J Neurosci. 21:6321-6328.